



Effectiveness of oil displacement by sequential low-salinity waterflooding in low-permeability fractured and non-fractured chalky limestone cores

Abdulrazag Y. Zekri¹ · Benny A. Harahap¹ · Hazim H. Al-Attar¹ · Essa G. Lwisa¹

Received: 18 February 2018 / Accepted: 10 May 2018 / Published online: 31 May 2018
© The Author(s) 2018

Abstract

Low-salinity waterflooding has been recognized as a method of enhancing oil recovery in low-permeability reservoirs. This method is relatively inexpensive and can be easily implemented in the field. Various mechanisms of low-salinity flooding have been proposed including interfacial tension reduction, wettability alteration (cation exchange), change in pH (increase), emulsion formation, and clay migration. Hydraulic fracturing has been known as a technique of stimulating hydrocarbon flow from low-permeability matrix into wellbores by creating high-conductivity fractures. The objective of this study is to evaluate the effectiveness of sequential low-salinity brine flooding process to enhance oil recovery in low-permeability fractured and non-fractured chalky limestone core samples. The low-salinity waterflooding tests were conducted with synthetic brines of five different salinity concentrations, namely, 157,662, 72,927, 62,522, 6252, and 1250 ppm. The properties of these brines have been thoroughly investigated in the laboratory. The crude oil and chalky limestone core samples, permeability range between 0.01 and 1.2 millidarcy, were gathered from a selected oil field in United Arab Emirates. When used as an opening move in a three-stage sequential brine flooding (SW/10→SW/50→SW $6 \times \text{SO}_4^{-2}$), sea water diluted ten times at 6252 ppm (SW/10) has been found to yield the highest oil recovery in fractured and non-fractured tests at the prevailing reservoir conditions, of 82.64 and 76% of OOIP, respectively. In all sequential brine flooding scenarios tested, sea water with sulfate concentration spiked six times (SW $6 \times \text{SO}_4^{-2}$) only slightly increased oil recovery. The highest observed incremental recovery with sulfate spiking was 2.083% of OOIP. The effectiveness of oil displacement by sequential brine flooding has been attributed to mineral dissolution and fines migration which resulted in a favorable wettability alteration. This postulation of flow mechanism is confirmed by introducing a “flow resistance index” concept and measurements of key properties of the injected and effluent brines of each stage of the attempted sequential brine flooding scenarios. Results of this study could be consulted when selecting most efficient EOR method to develop tight carbonate oil reservoirs in the UAE and worldwide.

Keywords Enhanced oil recovery · Low-permeability · Carbonate reservoir · Low-salinity waterflooding · Hydraulic fracturing

Background

The world energy demand is not static and it is forecasted to increase rapidly. Although the world is rapidly moving in the direction of using a mix of energy, it is expected that 53% of the world's energy needs will be met by oil and gas in 2040 (Ban et.al. 2016). Therefore, we can safely say

that oil will be a major player for the energy market for the next 30 years at least. Carbonate reservoirs contribute more than 60% of the world's petroleum production. Carbonate reservoirs (limestone or dolomite) are heterogeneous and require major skills to understand and develop a detailed reservoir description. Low-permeability carbonate reservoirs have been considered uneconomical to develop because of their low flow rates and longer pay out times. Oil in low-permeability oil reservoirs is classified as unconventional reserves. Unconventional reserve is defined by the oil industry as ‘hard to recover’ oil. The definition ‘hard to recover’ reserve includes reservoirs having low-permeability and/or porosity. The oil recovery by waterflooding technology is not

✉ Hazim H. Al-Attar
hazim.alattar@uaeu.ac.ae

¹ Chemical and Petroleum Engineering Department, UAE University, P.O. Box 15551, Al Ain, UAE

known as an effective method in low-permeability carbonate oil reservoirs. To maximize the wellbore–reservoir contact area in these low-permeability reservoirs, a number of oil companies completed horizontal wells with multiple hydraulic fracturing stages. In spite of above-mentioned technological advances, low-permeability oil reservoirs exhibit a huge variety of geological characteristics that makes the application of a single technique (completion/development) unrealistic and might lead to unfavorable economical and/or technical conditions. Therefore, an innovative exploration/exploitation strategy is required for optimal hydrocarbon recovery from low-permeability oil reservoirs. Consequently, research has been directed to develop new methods to improve oil recovery from this type of reservoirs.

In this work, we have investigated the possibility of using low-salinity, sequential low-salinity waterflooding, fracturing, and combination of sequential low-salinity flooding with hydraulic fracturing to improve oil recovery from low-permeability carbonate reservoirs. The objective is to determine the optimum technique for a selected low-permeability carbonate oil reservoir.

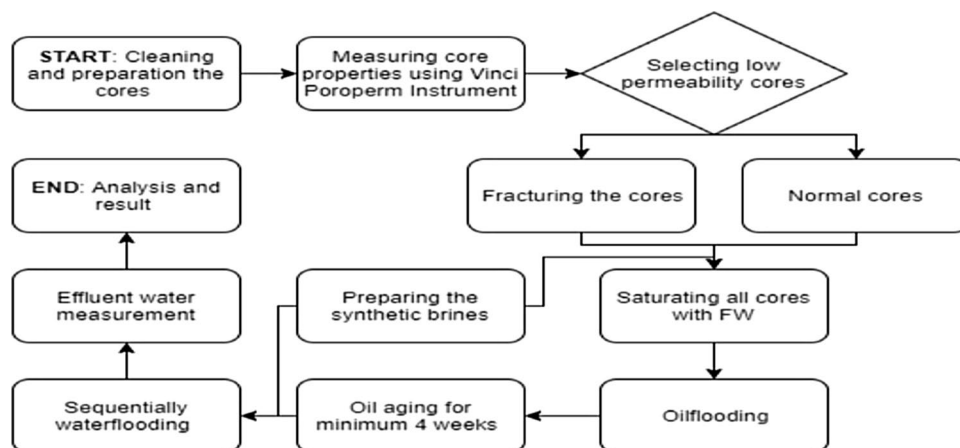
A substantial amount of research work has been conducted on the possibility of using low-salinity waterflooding in recovering oil from conventional sandstone and carbonate oil reservoirs Al-Quraishi et al. (2015). Al-Harrasi et al. (2012) investigated the performance of low-salinity using carbonate rocks and reported a significant oil recovery up to 16% of original oil in place. Al-Attar et al. (2013) investigated the effect of divalent ion concentration of the performance of low-salinity waterflooding and they concluded that sulfate concentration plays a major role on flood performance. Bagci et al. (2001) used dilutions of formation brine as injection system and they reported a success story in limestone rocks. Austad et al. (2010) indicated that fine migration is a major player in performance of low-salinity in carbonate oil reservoirs. Yi and Sarma (2012) reported that multi-ionic exchange concept is the mechanism in both sandstone and carbonate

keeping in mind that the process in carbonate reservoirs is quite different from that in sandstone reservoirs. Zekri et al. (2011) reported that wettability alteration is the dominant mechanism in both sandstone and carbonate rocks. Alameri et al. (2015) reported that the low-salinity waterflood in low-permeability carbonate rocks yielded incremental oil recovery of up to 9%. Alameri is the only author to our knowledge investigated the possibility of using low-salinity in low-permeability rocks. Comprehensive review on the mechanism of low-salinity flooding was conducted by Sheng (2014). He reported based on the literature review that several mechanism responsible for the success of low-salinity flooding. Although there are no clear consensus on the process mechanism, the majority attributed the improvement of oil recovery to wettability alteration. Other mechanism includes interfacial tension reduction, rock dissolution, ionic exchange, and oil emulsion also reported as possible mechanism. In most of the cases, it seems no single mechanism is responsible for the improvement of oil recovery by low-salinity flooding, but rather a combination of previously mentioned mechanism acting at different degrees.

Experimental procedures and materials

The experimental setup used in this work is designed to perform coreflooding tests by sequential brine injection with and without simulated induced single fracture. A flow chart demonstrating the sequence of the laboratory tests performed in this study is shown in Fig. 1. All flooding scenarios were conducted at simulated reservoir temperature and pressure. All materials including crude oil, core samples, and composition of injected water were provided by Abu Dhabi Company for Onshore Petroleum Operations Ltd. (ADCO).

Fig. 1 Flowchart illustrating the sequence of laboratory tests



Crude oil

Sweet crude oil sample with API gravity of 39.48 degrees is collected from Asab Field. This field is one of the five major fields operated by ADCO. The viscosity of this crude oil is 2.927 cp under ambient conditions and 1.8953 cp under 255F and 3100 psia.

Brines

Five brines were used in this study including formation water of Asab Field (FW), seawater (SW), seawater diluted 10 times (SW/10), seawater diluted 50 times (SW/50), and seawater with sulfate concentration spiked 6 times (SW $6 \times \text{SO}_4^{-2}$). The compositions of these five brines are listed in Table 1 and their densities and viscosities at ambient conditions are presented in Table 2.

Core samples

Nine chalky limestone (CaCO_3) core samples from Zakum Oil Field were used in this work. The results of their routine core analysis are presented in Table 3.

Simulating hydraulically induced fractures

The induced fracture was synthetically created by cutting the core sample into equal halves along the entire length of the core and as illustrated in Fig. 2. Aluminum foil was then placed between the core two halves to keep the simulated fracture face open and the outer surface area of the core was wrapped up with aluminum foil to keep the core intact. Four core samples were prepared this way, namely ZK-454-6F, ZK-454-11F, ZK-454-20F, and ZK-454-27F. The results of liquid permeability measurements of these core samples before and after fracture simulation are presented in Table 4.

Oilflooding and aging process

All core plugs were fully saturated with formation water and then flooded with oil to S_{wi} , then aged for 5 weeks. The results of this part of the experimental work are listed in Table 5.

Sequential waterflooding tests

These tests represent the major part of this study. It was intended to assess selected brines as potential fluids to enhance oil recovery under simulated reservoir conditions. Flooding tests were conducted sequentially starting with high salinity brines followed by lower salinities and sulfate

Table 1 Compositions of the five brines

Ion	FW		SW		SW/10		SW/50		SW $6 \times \text{SO}_4$	
	TDS (mg/l)	Salinity (ppm)	TDS (mg/l)	Salinity (ppm)	TDS (mg/l)	Salinity (ppm)	TDS (mg/l)	Salinity (ppm)	TDS (mg/l)	Salinity (ppm)
Sodium	44,261	44,312	19,054	19,076	1905	1908	381	382	24,137	24,165
Calcium	13,840	13,856	690	691	69	69	14	14	690	691
Magnesium	1604	1606	2132	2134	213	213	43	43	2132	2134
Potassium	0	0	672	673	67	67	13	13	672	673
Chloride	96,560	96,670	35,836	35,877	3584	3588	717	718	35,836	35,877
Bicarbonate	332	332	123	123	12	12	2	2	123	123
Sulfate	885	886	3944	3949	394	395	79	79	9254	9265
Total	157,482	157,662	62,451	62,523	6245	6252	1249	1250	72,844	72,928

Table 2 Density and viscosity of the five brines

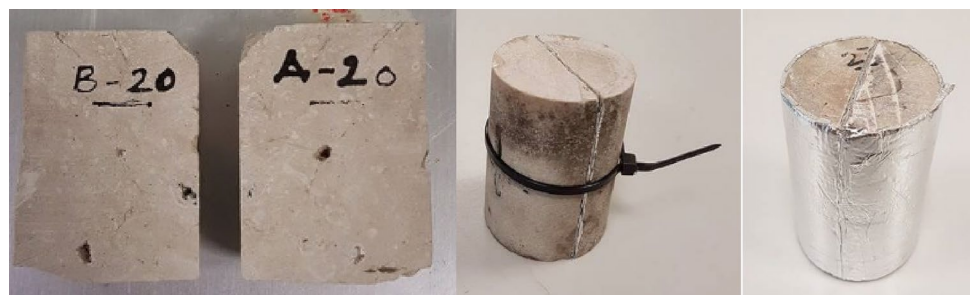
No.	Brine	Density (g/ml)	Viscosity (cP)
1	FW	1.103	1.35
2	SW	1.034	1.19
3	SW/10	1	1.07
4	SW/50	1	1.03
5	SW $6 \times \text{SO}_4^{2-}$	1.05	1.26

spiked using the coreflooding system setup as shown in Fig. 3. The sequential brine flooding scenarios of the nine core samples used in this work are presented in Table 6.

All the tests were conducted under similar reservoir conditions, an overburden pressure of 2500 psia (applied using the hydraulic pump) and temperature of 90 °C (core holder is equipped with a heating jacket). The injection rate of brines was kept constant at 1 cc/min throughout each sequential flooding scenario. A back pressure regulator was installed to control the outlet pressure at 100 psi to regulate the flow and avoid extra pressure build-up after heating the system. During each sequential flooding scenario, the salinity, resistivity, pH, and conductivity of the effluent water were measured. Salinity in ppm and resistivity in ohm.meter were measured using a digital resistivity meter. Conductivity (mS/cm) and pH values were measured using a digital conductivity meter and digital pH meter, respectively.

Table 3 Results of routine core analysis of the nine samples

Sample id	Dry wt (gm)	Length (cm)	Diameter (cm)	Pore vol. air (cc)	Bulk vol. (cc)	Grain vol. air (cc)	Grain den. (gm/cc)	Porosity air (%)	Permeability	
									Air (md)	Liquid (md)
ZK-454-2	171.93	6.818	3.801	13.45	77.4	63.94	2.69	17.4	0.15	0.09
ZK-454-3	174.4	6.932	3.803	13.7	78.77	65.07	2.68	17.4	0.25	0.16
ZK-454-4	175.95	7.103	3.794	14.48	80.33	65.85	2.67	18	0.24	0.15
ZK-454-5	169.77	6.998	3.801	15.8	79.44	63.64	2.67	19.9	1.06	0.73
ZK-454-6	135.81	5.418	3.812	10.86	61.86	51	2.66	17.5	0.49	0.32
ZK-454-11	124.35	5.305	3.793	13.95	59.97	46.02	2.7	23.3	0.02	0.01
ZK-454-13	141.22	6.234	3.801	18.43	70.77	52.33	2.7	26	0.98	0.66
ZK-454-20	125.13	5.279	3.806	13.66	60.08	46.43	2.7	22.7	0.05	0.03
ZK-454-27	131.59	5.684	3.8	15.7	64.49	48.79	2.7	24.3	1.7	1.2

Fig. 2 Simulating a single induced fracture**Table 4** Liquid permeability before and after fracturing

Core no	Permeability liquid(mD)		Folds of permeability increase
	Initial	Fractured	
ZK-454-6F	0.32	2.23	7.0
ZK-454-11F	0.02	6.97	348.3
ZK-454-20F	0.02	3.02	150.8
ZK-454-27F	1.7	3.88	2.3

Results and discussion

During each stage of the attempted sequential waterflooding scenarios, the volumes of the produced and injected fluids as well as the pressure drop across the core were carefully and continuously measured as a function of time. Due to space limitation, the results of one sequential brine flooding scenario of the non-fractured core ZK-454-3 are presented in Table 7 and Fig. 4. A complete set of all the results of this work can be found in Benny (2017).

In addition to the above and for the same core sample, the end-point effective permeability to brine of each flooding stage within the above sequential flood scenario (k_{weff}) was calculated using Darcy's equation at residual oil residual (S_{or}). The viscosity of various brines at 90 °C was estimated using an empirical correlation developed

Table 5 Results of flooding core samples to S_{wi}

No.	Core ID	Length (cm)	Diameter (cm)	Pore Vol by water (cc)	Porosity by water (%)	Permeability by water (md)	Produced Water (cc)	Swi	Soi
1	ZK-454-2	6.818	3.801	11.818	15.276	0.09	9.5	0.196	0.804
2	ZK-454-3	6.932	3.803	11.628	14.767	0.16	9.1	0.217	0.783
3	ZK-454-4	7.103	3.794	12.244	15.247	0.15	10	0.183	0.817
4	ZK-454-5	6.998	3.801	13.622	17.154	0.73	11.3	0.170	0.830
5	ZK-454-13	6.234	3.801	15.688	22.178	0.66	11.5	0.267	0.733
6	ZK-454-6F	5.418	3.862	9.075	14.299	2.23	7	0.229	0.771
7	ZK-454-11F	4.619	3.843	9.888	18.455	6.97	7.2	0.272	0.728
8	ZK-454-20F	4.703	3.856	9.045	16.469	3.02	7.4	0.182	0.818
9	ZK-454-27F	5.684	3.850	12.416	18.764	3.88	10	0.195	0.805

Fig. 3 Schematic of coreflooding experimental set up; v1, v2, and v3 are isolation valves

A SKETCH FOR WATER AND OIL FLOODING SYSTEM AT RESERVOIR CONDITIONS

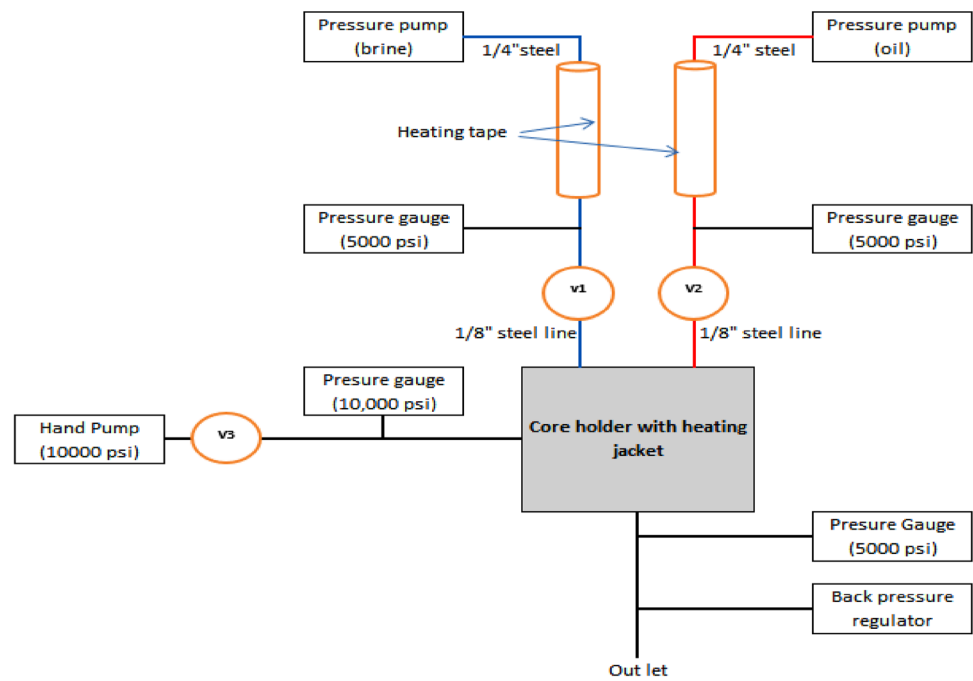


Table 6 Sequential waterflooding scenarios

No.	Sample id	Order of brines injected				
		1st	2nd	3rd	4th	5th
1	Z K-454-2	SW	SW/10	SW/50	SW 6×SO ₄ ²⁻	
2	Z K-454-3	FW	SW	SW/10	SW/50	SW 6×SO ₄ ²⁻
3	Z K-454-4	SW/10	SW/50	SW 6×SO ₄ ²⁻		
4	Z K-454-5	SW/50	SW 6×SO ₄ ²⁻			
5	Z K-454-13	SW 6×SO ₄ ²⁻	SW/50			
6	Z K-454-6F	FW	SW	SW/10	SW/50	SW 6×SO ₄ ²⁻
7	Z K-454-11F	SW/10	SW/50	SW 6×SO ₄ ²⁻		
8	Z K-454-20F	SW	SW/10	SW/50	SW 6×SO ₄ ²⁻	
9	Z K-454-27F	SW 6×SO ₄ ²⁻	SW/50			

Table 7 Results of sequential flooding scenario of a non-fractured core sample ZK-454-3

No.	Injected Brines	Voil produced (cc)	Vwater Injected (cc)	Incremental RF (%)	RF (%)	Incremental PV injected	PV injected
1	FW	0	0	0.000	0.000	0.000	0.000
		3.9	6.1	42.857	42.857	0.860	0.860
		0.8	9.2	8.791	51.648	0.860	1.720
		0.4	9.6	4.396	56.044	0.860	2.580
		0.2	9.8	2.198	58.242	0.860	3.440
		0.1	9.9	1.099	59.341	0.860	4.300
2	SW	0	9.4	0.000	59.341	0.808	5.108
		0.6	17.3	6.593	65.934	1.542	6.651
3	SW/10	0	34.7	0.000	65.934	2.981	9.632
		0.3	17.4	3.297	69.231	1.525	11.157
4	SW/50	0	34.9	0.000	69.231	2.999	14.156
		0.2	17.4	2.198	71.429	1.511	15.667
5	SW 6×SO ₄ ²⁻	0	34.7	0.000	71.429	2.987	18.654
		0.1	17.5	1.099	72.527	1.509	20.163
		0	34.9	0.000	72.527	3.001	23.164

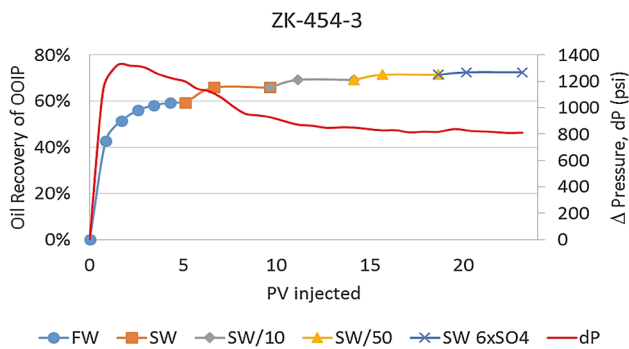


Fig. 4 Oil recovery as per cent of OOIP and pressure drop across versus PV injected for core sample ZK-454-3

by El-dessouky (2002). The results of end-point effective permeability calculations are shown in Fig. 5.

Sequential low-salinity waterflooding of non-fractured cores

A summary of the results of sequential coreflooding scenarios of non-fractured core samples is shown in Table 8. By comparing the results of cores ZK-454-2 and ZK-454-3, it can be sated that less volume of injected brines is required to recover approximately the same amount of oil without the injection of FW. All sequential flooding scenarios were conducted at a constant injection rate of 1 cc/min. The pressure drop at S_{or} was recorded for each stage of every sequential scenario as presented in Table 8. A general trend of declining pressure drop can be observed with decreasing brine salinity. Such a trend is indicative

Fig. 5 End-point effective permeability to brines of the sequential flood scenario of the non-fractured core sample ZK-454-3

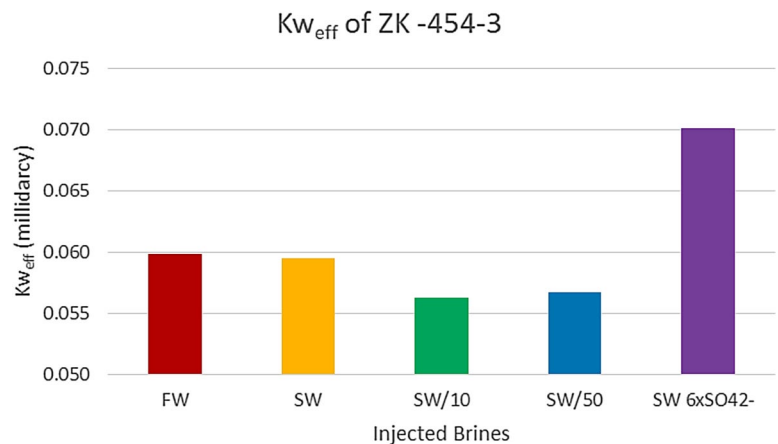
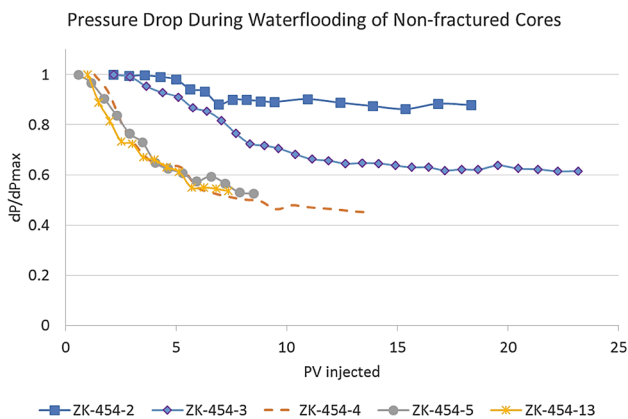


Table 8 Summary of results of sequential flooding scenarios of non-fractured core samples

No.	Core ID	Injected Brines	Voil Produced (cc)	V _{water} Injected (cc)	Incremental RF (%)	RF	Incremental PV injected	PV injected	AP at S _{or} (psi)	K _{w,eff} at S _{or} estimated (millidarcy)
1	ZK-454-2	SW	6.1	59.1	64.211	64.211	5.001	5.001	1250	0.044
		SW/10	0.3	52.6	3.158	67.368	4.451	9.452	1136	0.041
		SW/50	0.25	52.35	2.632	70.000	4.430	13.881	1115	0.041
		SW 6×SO ₄ ²⁻	0.15	52.55	1.579	71.579	4.447	18.328	1120	0.050
2	ZK-454-3	FW	5.4	59.4	59.341	59.341	5.108	5.108	1200	0.060
		SW	0.6	52.6	6.593	65.934	4.524	9.632	930	0.060
		SW/10	0.3	52.6	3.297	69.231	4.524	14.156	851	0.056
		SW/50	0.2	52.3	2.198	71.429	4.498	18.654	818	0.057
3	ZK-454-4	SW 6×SO ₄ ²⁻	0.1	52.45	1.099	72.527	4.511	23.164	811	0.070
		SW/10	7.2	64	72.000	72.000	5.227	5.227	1105	0.045
		SW/50	0.3	52.5	3.000	75.000	4.288	9.515	811	0.059
		SW 6×SO ₄ ²⁻	0.1	52.5	1.000	76.000	4.288	13.803	788	0.074
4	ZK-454-5	SW/50	8.1	63.1	71.681	71.681	4.632	4.632	381	0.123
		SW 6×SO ₄ ²⁻	0.2	52.7	1.770	73.451	3.869	8.501	320	0.180
5	ZK-454-13	SW 6×SO ₄ ²⁻	7.4	63	64.348	64.348	4.016	4.016	513	0.100
		SW/50	0.45	52.6	3.913	68.261	3.353	7.369	415	0.101

**Fig. 6** Flow resistance index versus pore volume injected of five sequential scenarios of brines flooding in non-fractured systems

of improved oil displacement by low-salinity brines. The improved effectiveness of low-salinity brines in displacing oil may be attributed to mineral dissolution and thus improved alteration of wettability to the more favorable water-wet status.

Also shown in Table 8 is that the highest recovery factor was achieved in sequential number 3. Results of end-point effective permeability at S_{or} at the end of each stage of a certain sequential flooding scenario indicate a shift of $K_{w,eff}$ to higher values. This shift supports the wettability alteration as being the dominant mechanism which is responsible for the improved oil recovery. Spiking of SW with SO_4^{2-} improved the oil recovery by 3%.

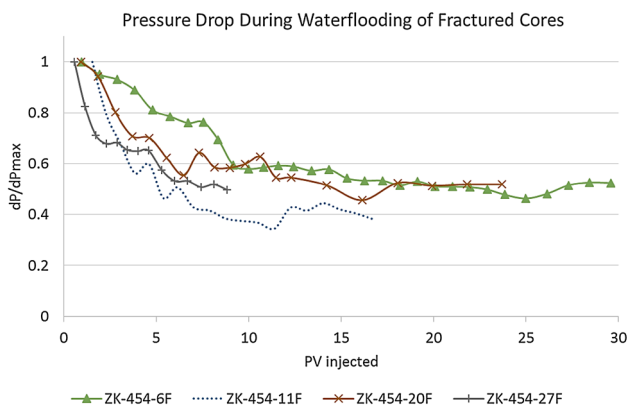
Figure 6 presents a proposed flow resistance index as a function of pore volumes of injected brine. During any scenario of sequential brine flooding, the flow resistance index is defined as the ratio of pressure drop across the core sample to the maximum pressure drop across the core. These results show that sequential scenario number 3 is one of three sequential flooding scenarios which exhibited a significant reduction of the flow resistance index. This observation confirms our previous postulation regarding alteration of wettability as being the dominant mechanism that contributes to improved oil recovery.

Sequential low-salinity waterflooding in fractured cores

Many operators believe that development of tight oil reservoirs can only be achieved by hydraulic fracturing. In this section, the performance of sequential brine flooding in core samples with synthetic fractures is evaluated and compared with that of the non-fractured systems. A Summary of the results of sequential coreflooding by various brines in four fractured cores under simulated reservoir conditions of pressure and temperature are presented in Table 9. By comparing the results presented in Tables 8 and 9 and the results shown in Fig. 6, and for similar sequential scenarios of brine flooding, it is clear that there is a significant increase of oil recovery in fractured cores. For example, a 5% additional oil recovery could be obtained when using the SW/10 brine in fractured system over the non-fractured system. The optimum sequential scenario of brine flooding in fractured cores

Table 9 Summary of results of sequential brine flooding scenarios in synthetically fractured cores

No.	Core ID	Injected Brines	Voil produced (cc)	Vwater injected (cc)	Incremental RF (%)	RF (%)	Incremental PV injected	PV injected	AP at Sor (psi)	$K_{w_{eff}}$ at Sor estimated (mildarcy)
1	ZK-454-6F	FW	4.6	60.9	65.714	65.714	6.711	6.711	413	0.135
		SW	0.45	51.85	6.429	72.143	5.713	12.424	320	0.135
		SW/10	0.25	52.25	3.571	75.714	5.757	18.181	280	0.133
		SW/50	0.15	51.35	2.143	77.857	5.658	23.840	260	0.139
		SW $6 \times SO_4^{2-}$	0.1	52.1	1.429	79.286	5.741	29.580	285	0.155
2	ZK-454-11F	SW/10	5.55	60.75	77.083	77.083	6.144	6.144	289	0.111
		SW/50	0.25	51.75	3.472	80.556	5.234	11.378	197	0.158
		SW $6 \times SO_4^{2-}$	0.15	52.05	2.083	82.639	5.264	16.642	219	0.174
3	ZK-454-20F	SW	5.3	58.6	71.622	71.622	6.479	6.479	313	0.120
		SW/10	0.3	52.6	4.054	75.676	5.815	12.294	308	0.105
		SW/50	0.1	52	1.351	77.027	5.749	18.043	296	0.106
		SW $6 \times SO_4^{2-}$	0.1	51.1	1.351	78.378	5.650	23.693	293	0.131
4	ZK-454-27F	SW $6 \times SO_4^{2-}$	6.75	56.85	67.500	67.500	4.579	4.579	299	0.156
		SW/50	0.4	52.7	4.000	71.500	4.244	8.823	228	0.167

**Fig. 7** Flow resistance index versus pore volumes of injected brines in fractured systems

is number 2 for core ZK-454-11F (SW/10→SW/50→SW $6 \times SO_4^{2-}$) which resulted in oil recovery of 82.639% of the OOIP. Fractured and non-fractured systems, however, share similar optimum brine flooding of SW/10.

As depicted in Fig. 7, a plot of the flow resistance index versus pore volumes of injected brine exhibits similar trends as for the non-fractured systems. Similar trends of end-point effective permeabilities are also observed for both systems. Therefore, similar conclusions may be drawn regarding the mechanism responsible for improved oil recovery, i.e., mineral dissolution that leads to a more favorable wetting characteristics.

The results of all scenarios of sequential brine flooding tests in fractured and non-fractured core samples are illustrated in Fig. 8. It can be stated that using the SW/10

brine in the secondary recovery mode in fractured cores is found to yield the highest oil recovery of 82.64% of the original OOIP.

Monitoring brines' properties

Brine water properties including salinity, resistivity, conductivity, pH, and TDS before and after each stage of each sequential brine flooding scenario were measured. The results of such measurements of one scenario of sequential brine flooding are presented in Table 10. Total TDS of the effluent water was calculated using a reliable TDS converter software developed by Chemia-soft which converts brine conductivity to TDS. These results show that the maximum mineral dissolution is observed during SW/10 brine flooding stage as the TDS was increased by 295%. This observation also confirms our previously mentioned postulation of mineral dissolution which could have changed rock surface properties to the favorable wettability characteristics. These findings are in line with those obtained by Zahid et.al. (2012).

As indicated in Table 10, when the salinity of the effluent water increases, the resistivity will decrease and so will the conductivity. Measurements of the pH values, in fact, show that there is a correlation between the above properties. No significant change in the pH value was observed during the SW/10 stage. Other stages of sequential flooding such as flooding with SW/50 displayed an increase in pH value. Consequently, no clear conclusion regarding the recovery mechanism can be drawn based on these results.

Fig. 8 Results of sequential brine flooding tests of all scenarios

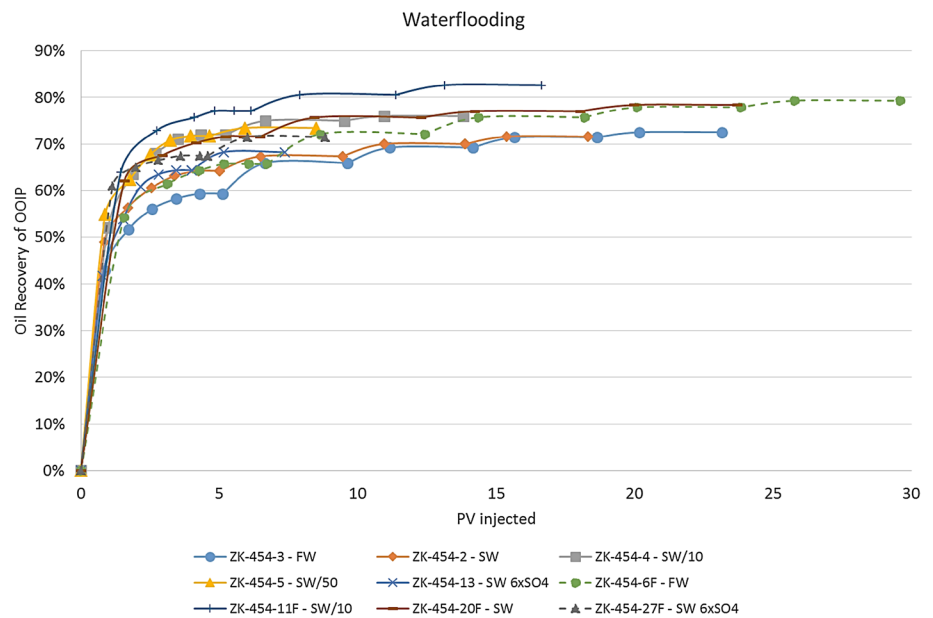


Table 10 Results of measurements of supportive brine water properties of one scenario of sequential brine flooding

Injected Water	Salinity (ppm)		Resistivity (ohm*meter)		Conductivity (mS/cm)		pH		TDS (mg/L)	
	Before	After	Before	After	Before	After	Before	After	Before	After
FW	157,662	117,314	0.068	0.071	197.2	189.5	7.12	6.98	157,482	123,322
SW	62,522	69,259	0.136	0.104	89.9	125.3	7.22	6.89	62,451	83,779
SW/10	6252	20,584	1	0.291	11.63	40	7.17	7.18	6245	24,673
SW/50	1250	4496	3.53	1.21	3.13	9.47	7	7.33	1249	5446
SW 6xSO ₄ ²⁻	72,927	56,565	0.133	0.174	90	71	7.35	7.23	72,844	59,194

Conclusions

Based on the results of this work the following conclusions can be drawn:

1. Sequential flooding scenarios which begin with the injection of sea water diluted ten times (SW/10) have been found to yield highest oil recoveries. In non-fractured core samples, the highest oil recovery was 76% of OOIP and was achieved with the sequential flooding scenario which begins with SW/10 followed by SW/50 followed by SW 6xSO₄²⁻ (Table 8). In fractured core samples, the highest reported oil recovery was 82.64% of OOIP and was achieved with the sequential flooding scenario which begins with SW/10 followed by SW/50 followed by SW 6xSO₄²⁻ (Table 9).
2. Adding divalent sulfate ion to low-salinity water would increase the overall cost of the oil recovery process and may not necessarily improve the effectiveness of oil displacement by the low-salinity water.

3. It is postulated that mineral dissolution and favorable shift of end-point effective permeability could lead to a more favorable wettability condition. This mechanism of oil displacement by sequential brine flooding has been confirmed by monitoring “flow resistance index” proposed in this work and measuring key properties of brine water before and after sequential flooding.

Acknowledgements Financial support and samples of this work are gratefully acknowledged from the Abu Dhabi Company for Onshore Petroleum Operations Ltd. (ADCO), Contract No. 21R011-The Petroleum Institute. Also authors would like to thank UAE U research sector for their support.

Open Access This article is distributed under the terms of the Creative Commons Attribution 4.0 International License (<http://creativecommons.org/licenses/by/4.0/>), which permits unrestricted use, distribution, and reproduction in any medium, provided you give appropriate credit to the original author(s) and the source, provide a link to the Creative Commons license, and indicate if changes were made.

References

- Alameri W, Teklu TW, Graves RM, Kazemi H, AlSumaiti AM (2015) Experimental and numerical modeling of low-salinity waterflood in a low-permeability carbonate reservoir. Paper SPE-174001-MS. SPE Western regional Meeting, California
- Al-Attar HH, Mahmoud MY, Zekri AY, Almehaideb R, Ghannam M (2013) Low-salinity flooding in a selected carbonate reservoir: experimental approach. *J Pet Explor Prod Technol* 3(2):139–149. <https://doi.org/10.1007/s13202-013-0052-3>
- Al-Harrasi A, Al-maamari RS, Masalmeh SK (2012) Laboratory investigation of low-salinity waterflooding for carbonate reservoirs. *Soc Pet Eng*. <https://doi.org/10.2118/161468-MS>
- Al-Quraishi AA, Al Hussinan SN, Al Yami HQ (2015). Efficiency and recovery mechanisms of low-salinity waterflooding in sandstone and carbonate reservoir. In: Proceedings of the Offshore Mediterranean Conference and Exhibition, OMC-2015- 223, Ravenna, Italy
- Austad T, RezaeiDoust A, Puntervold T (2010) Chemical mechanism of low-salinity water flooding in sandstone reservoirs. Paper SPE129767 presented at the SPE Improved Oil Recovery Symposium. Tulsa, OK, 24–28 Apr 2010
- Bagci S, Kok MV, Turksoy U (2001) Effect of brine composition on oil recovery by waterflooding. *Pet Sci Technol*. 19(3–4):359–372. <https://doi.org/10.1081/LFT-100000769>
- Ban J, Arellano JL, Alawami A, Aguilera RF, Tallett M (2016) World Oil Outlook. Organization of the Petroleum Exporting Countries
- Benny A, Harahap (2017) Laboratory investigation of oil recovery efficiency achieved by low-salinity waterflooding in low-permeability fractured and non-fractured chalky limestone cores, M.Sc. Thesis submitted to the College Of Engineering, Chemical & Petroleum Engineering Department, UAE University, Dec 2017
- El-Dessouky HT, Ettouney HM (2002) Fundamentals of sea water desalination. Elsevier, Amsterdam
- Sheng JJ (2014) Critical review of low-salinity water flooding. *J Pet Sci Eng* 120:216–224. <https://doi.org/10.1016/j.petrol.2014.05.026>
- Yi Z, Sarma HK (2012) Improving waterflood recovery efficiency in carbonate reservoirs through salinity variations and ionic exchanges: a promising low-cost ‘Smart-Waterflood’ approach. In: Proceedings of the Abu Dhabi International Petroleum Conference and Exhibition, SPE-161631-MS, Abu Dhabi, UAE
- Zahid A, Shapiro AA, Skauge A (2012) Experimental studies of low-salinity waterflooding carbonate: a new promising approach. In: Proceedings of the SPE EOR Conference at Oil and Gas West Asia, SPE-155625-MS, Muscat, Oman
- Zekri AY, Nasr MS, Al-Arabai ZI (2011) Effect of losal on wettability and oil recovery of carbonate and sandstone format ion. *Int Pet Technol Conf*. <https://doi.org/10.2523/IPTC-14131-MS>

Publisher’s Note Springer Nature remains neutral with regard to jurisdictional claims in published maps and institutional affiliations